THE UNIVERSITY OF MICHIGAN

INDUSTRY PROGRAM OF THE COLLEGE OF ENGINEERING

HYDRAULIC JUMP IN A ROTATING FLUID

Chia-Shun Yih
H. E. Gascoigne
W. R. Debler

April, 1963

IP-613

ACKNOWLEDGMENTS

This work has been sponsored jointly by the National Science Foundation and the Army Research Office (Durham). The authors wish to express their appreciation for this sponsorship, and their thanks to Dr. David Appel for helping in the measurement of the upstream depth.

LIST OF TABLES

LIST OF FIGURES

LIST OF PLATES

1. INTRODUCTION

It has been generally recognized that the flows of a rotating fluid are, in many respects, similar to the flows of a stratified fluid in the presence of a gravitational field. Since a free surface is a surface of density discontinuity, which is a form of extreme stratification, there is also a similarity of flows of a rotating fluid with a free surface to free-surface flows in the gravitational field. A free surface in the rotating fluid is necessary to ensure similarity of its flow to a free-surface flow in the gravitational field because the quantity corresponding to a discontinuity in specific weight in the latter is a discontinuity in $\rho \Gamma^2$ in the former, ρ being the density and Γ the circulation of the flow along any circle in its domain located with axial symmetry. Thus the counterpart of the ordinary hydraulic jump appears to be a hydraulic jump in a layer of liquid flowing down the inner wall of a rotating cylinder, and rotating with it.

The analysis was carried out in 1961 and construction of the apparatus for experimentation started in October of that year. By the summer of 1962 the phenomenon was clearly observed in a repeatable fashion in the apparatus constructed. When this was mentioned to Mr. A. M. Bonnie of Cambridge University, who was visiting the first author in September of 1962, Mr. Bonnie showed some pictures of a hydraulic jump he observed in a swirling flow down a stationary tube, in an experiment performed to study the effect of a bend on a swirling fluid. His work has since been published [1]. But his tube is stationary and his work is not primarily a study of hydraulic jump in a rotating fluid.

Due to the difficulty involved in the measurement of the upstream thickness of the water layer, the experiments were finished only in December, 1962. The analytical and experimental results are presented in this paper to provide yet another instance of the similarity of rotating flows and stratified flows.

2. ANALYSIS

With reference to Figure 1, b is the inner radius of the tube, d_1 is the depth of water upstream from the jump, and d_2 the downstream depth. The pressure in the fluid upstream from the jump is

$$p_1 = \frac{\rho\omega_1^2}{2} (r^2 - a_1^2) , \qquad (\omega_1 = \omega) \tag{1}$$

in which ω_1 is the angular speed of the rotating water film, and is equal to the angular speed ω of the rotating cylinder, r is the radial distance from the axis to the point at which the pressure is being considered, and $a_1 = b - d_1$. Downstream from the jump, the angular speed of the fluid ω_2 in general varies from one radial position to another. Two extreme situations may be considered. If viscous and turbulent mixings are ignored, Kelvin's theroem on the conservation of circulation enable one to compute ω_2 as a function of r, upon utilization of the equation of continuity and the assumption that the downstream velocity U_2 is constant. This would be a very unrealistic situation, because there is violent turbulent mixing at the jump, so that Kelvin's theorem cannot be valid. The other extreme condition is the condition of complete mixing, so that after the jump another uniform ω_2 exists, which can be computed from ω_1 by use of the conservation of the integrated angular momentum. Thus, on the assumption that ω_2 is uniform, the downstream pressure distribution is given by

$$p_2 = \frac{\rho\omega_2^2}{2} (r^2 - a_2^2), \tag{2}$$

in which $a_2 = b - d_2$. The total axial force acting at an upstream section (Section 1-1) is

$$P_1 = \int_{a_1}^{b} p_1 \, 2\pi r dr = \frac{\rho\pi}{4} \omega^2 (b^2 - a_1^2)^2 . \tag{3}$$

The total axial force acting at downstream section (Section 2-2) is

$$P_2 = \int_{a_2}^{b} p_2 \, 2\pi r dr = \frac{\rho\pi}{4} \omega_2^2 (b^2 - a_2^2)^2 . \tag{4}$$

The discharge is given by

$$Q = \int_{a_1}^{b} U_1 \, 2\pi r dr = \int_{a_2}^{b} U_2 \, 2\pi r dr, \tag{5}$$

which is the equation of continuity. The downstream flow is very turbulent, so that U_2 can be assumed constant without appreciable error. If the upstream flow is also turbulent, so that U_1 can also be assumed constant, the equation of continuity can be written as

$$U_1(b^2 - a_1^2) = U_2 (b^2 - a_2^2). \tag{6}$$

The momentum flux through Section 1-1 is

$$M_1 = \int_{a_1}^{b} \rho U_1^2 \, 2\pi r dr, \tag{7}$$

and that through Section 2-2 is

$$M_2 = \int_{a_1}^{b} \rho U_2^2 \, 2\pi r dr. \tag{8}$$

If U_1 and U_2 are assumed constant,

$$M_1 = \rho\pi U_1^2 (b^2 - a_1^2), \text{ and } M_2 = \rho\pi U_2^2 (b^2 - a_2^2). \tag{9}$$

The fluxes of angular momenta are the same before and after the jump, since the torque exerted by the wall of the cylinder can be neglected.

Thus

$$\int_{a_1}^{b} (\rho\omega r^2)\ U_1\ 2\pi r dr = \int_{a_1}^{b} (\rho\omega_2 r^2)\ U_2\ 2\pi r dr. \qquad (10)$$

Now ω is constant, and as explained before U_2 and ω_2 can be assured constant. If the upstream flow is turbulent, U_1 can also be assumed constant, and (10) becomes

$$\rho\omega U_1\ (b^4 - a_1{}^4) = \rho\omega_2 U_2 (b^4 - a_2{}^4). \qquad (11)$$

which can be reduced to

$$\omega(b^2 + a_1{}^2) = \omega_2(b^2 + a_2{}^2) \qquad (12)$$

by the use of (6).

The momentum equation applied to the fluid between Sections 1-1 and 2-2 is

$$P_1 - P_2 + W = M_2 - M_1\ , \qquad (13)$$

in which W is the weight of the body of fluid in the region of change of depth. If the inner radius of that body of fluid is assumed to vary linearly (with 3) from a_1 to a_2, and if the length of the jump is assumed to be $c(a_1 - a_2)$, c being a constant of proportionality,

$$W = g\rho\pi(a_1 - a_2)\ (b^2 - \frac{a_1{}^2 + a_1\ a_2 + a_2{}^2}{3})$$

$$= g\rho\pi(a_1 - a_2)\ [b^2 - a_1\ a_2 - \frac{1}{3}\ (a_1 - a_2)^2]. \qquad (14)$$

Equation (13) then becomes

$$\frac{\rho\pi}{4}\,[\omega^2(b^2 - a_1{}^2)^2 - \omega_2{}^2(b^2 - a_2{}^2)] + g\rho\pi(a_1 - a_2)[b^2 - a_1\,a_2 - \frac{1}{3}(a_1 - a_2)^2] = \rho\pi[U_2{}^2(b^2 - a_2{}^2) - U_1{}^2(b^2 - a_1{}^2)]. \tag{15}$$

Now if (6) is used on the right-hand side, (12) is used to eliminate ω_2 and for simplicity one writes

$$\alpha_1 = \frac{a_1}{b},\ \alpha_2 = \frac{a_2}{b},\quad F_1 = \frac{U_1}{\omega b},\quad G = \frac{g}{b\omega^2}$$

One obtaines, after simplifications,

$$(1 - \alpha_1{}^2\alpha_2{}^2)(1 - \alpha_2{}^2) = F_1{}^2(1 - \alpha_1{}^2)(1 + \alpha_2{}^2) + \frac{c\,G\,(1 - \alpha_2{}^2)\,(1 + \alpha_2{}^2)^2\,[3(1 - \alpha_1\alpha_2) - (\alpha_1 - \alpha_2)^2]}{3(\alpha_1 + \alpha_2)} \tag{16}$$

This equaltion enables one to find α_2 for given values of α_1, F_1, G, and c.

In the experiments performed, d_1 and d_2 were very small compared with b. Hence a_1 and a_2 were nearly equal to b and so α_1 and α_2 were nearly equal to 1. Putting α_1 and α_2 equal to 1 except where differences are involved, one obtains from (16)

$$(1 - \alpha_1\alpha_2)(1 - \alpha_2) = 2\,F_1{}^2(1 - \alpha_1) + c\,G\,(1 - \alpha_2)\,[(1 - \alpha_1\alpha_2) - \frac{1}{3}(\alpha_1 - \alpha_2)^2]. \tag{17}$$

Now with

$$\eta = \frac{d_2}{d_1}\ ,\ \text{and}\ F^2 = \frac{U^2}{\omega^2 b d_1}$$

one has

$$1 - \alpha_1\alpha_2 = \frac{d_1}{b} (1 + \eta), \quad (1 - \alpha_2) = \frac{d_1}{b} \eta, \quad F_1^{\,2} (1 - \alpha_1) = F_1^{\,2} \frac{d_1}{b}$$

and

$$(\alpha_1 - \alpha_2)^2 = \frac{d_1^{\,2}}{b^2} (\eta - 1)^2.$$

Thus (17) can be written as

$$\eta(\eta + 1)(1 - c\, G) + \frac{1}{3} \frac{d_1}{b} c\, G\, \eta(\eta - 1)^2 = 2F^2. \qquad (18)$$

The depth ratio η had a maximum value of 10.7 in one test, and less than 10 on all the other tests, and d_1/b was very small. Thus, under the experimental conditions, the second term on the right-hand side can be neglected. The resulting equation can be solved simply. The solution is

$$\eta = \frac{d_2}{d_1} = \frac{1}{2} [-1 + \sqrt{1 + \frac{8F^2}{1 - c\, G}}]. \qquad (19)$$

3. APPARATUS AND METHOD OF MEASUREMENT

The apparatus is shown in Plate I and schematically in Figure 2. The working section was a piece of transparent tube of polished cast resin about 50 inches long and 9 inches in outside diameter. The thickness of the wall was 1/4 of an inch. The inner-surface diameter had a variation of at most 0.012 inch. The tube is supported by a rigid hub at the top and a rigid ring at the bottom. A rod running centrally from the top to the bottom carried a movable point gage for measuring depths. A turntable fixed to the bottom ring supporting the transparent tube was driven by a vanable-speed motor of 5 horsepower.

Water at 62° F was introduced into the tube through a rotating union threaded into the top hub from a head tank. The flow was regulated by needle valves through flow meters of the type of the Fischer-Porter rotometer. The flow meters were calibrated under test conditions and the variation of the discharge was within $\pm$ 1 per cent in each run. After entering the rotating union, the water was spread onto the inner wall of the best cylinder by a circular plate. Vertical uniform flow was established after approximately one tube diameter and a half.

At the bottom of the tube were efflux ports which could be opened or closed at will to adjust the location of the jump. The jump could be moved up the tube by reducing the opening at the bottom of the tube.

The angular speed of the turntable was measured electromagnetically and was maintained constant. The variation in each run was no more than 1 r.p.m., or about $\pm$ 0.1 per cent in the tests. This angular speed is the same as ω in the analysis. Plate II shows the location of the jump and streaks in the flow both upstream and downstream of the jump. Since ω was known and d_1 was small, the circumferential velocity upstream from the jump was known. Assuming the streaks were statistically the same as the streamlines, one could obtain the upstream surface velocity U_1 of the fluid in the axial direction from the inclination of the streaks. From U_1 one can easily calculate d_1. The mean inclination of the streaks was obtained photographically with a variation of $\pm$ 0.50. Downstream from the jump the inclination of the streaks were too small to be useful as a reliable means of obtaining d_2, which was therefore measured with the point gage. The error was with $\pm$ 0.007 inch approximately. The upstream depth was so small that the waviness of the free-surface would introduce a substantial percentage error in d_1 if measured with the point gage. That was why the streaks were utilized upstream from the jump.

The length of the jump was observed to be between 0.5 inch and 1 inch in the tests.

4. DISCUSSION OF RESULTS

The results are shown in Table 1 and Figure 3. As explained in Section 3, U_1 was computed from the inclination of the streaks on the upstream free surface. Since the upstream flow was assumed to be turbulent, this U_1 was considered to be the axial velocity in the major part of the upstream flow. The Reynolds member

$$R = \frac{U_1 d_1}{\nu}$$

based on the surface velocity was recorded in Table 1, with $\nu = 1.2 \times 10^{-5}$ ft^2/sec. The values of R show that the judgment of turbulent upstream flow is not an unrealistic one. It is known that plane Poiseuille flow, which would be the upstream flow if it were laminar and the slight curv ture effect were neglected, is unstable at a value 2000 for the Reynolds member based on the mean velocity, or 3000 for R. It is also known that a free surface tends to destabilize the flow. But it is important to remember the distinction between stability against surface waves and that against shear waves. For surface waves the flow is unstable at any Reynolds number however small, but at the same time it is shear-wave instability that is responsible for turbulence. In view of the fact that the Reynolds numbers recorded are from 930 to 2400, which are of the order of 3000, and considering that the flow was not free from turbulence as it entered the tube, the assumption of turbulent upstream flow was not unrealistic. With Q as the discharge in in^3/sec. d_1 in inches was obtained from

$$d_1 = 0.0375\ Q/U_1\ ;$$

U_1 being in in/sec.

In Figure 3 the data are plotted in a chart with F as the abscissa and d_2/d_1 as the ordinate. Equation (19) is plotted with $c = 0$, and also, for best fit at various values of G, for $c = 7$. This value for c is the same as for the length of the ordinary hydraulic jump. It can be seen that the agreement between the theoretical prediction and the experimental results is quite satisfactory.

TABLE 1

DATA FOR ROTATING HYDRAULIC JUMP

Run	rpm	Q in^3/sec	α deg	$\tan\alpha$	U_1 in/sec	d_1 in	d_2 in	F	$\frac{d_2}{d_1}$	R	$\frac{b\omega_1^2}{g}$
1	462	44.4	21	0.38	79	0.021	0.18	5.5	8.8	1400	25.8
2	535	42.2	19.8	0.36	86	0.018	0.16	5.5	8.9	1300	34.6
3	535	29.8	17	0.31	72	0.015	0.12	5.2	8.0	900	34.6
4	430	33.0	21	0.38	73	0.017	0.18	6.1	10.7	1000	22.4
5	540	44.4	19.7	0.36	86	0.019	0.16	5.3	8.1	1400	35.2
6	622	31.6	16	0.29	79	0.015	0.11	4.9	7.2	1000	47.1
7	592	32.8	16.3	0.29	77	0.016	0.11	4.7	6.9	1000	42.4
8	465	47.5	21	0.38	79	0.022	0.17	5.3	7.8	1500	26.2
9	565	47.5	18.8	0.34	86	0.021	0.15	4.9	7.2	1500	34.7
10	625	47.5	16.5	0.30	61	0.029	0.14	2.7	4.7	1500	47.2
11	455	53.3	23	0.42	86	0.023	0.21	5.7	9.2	1700	25.0
12	610	53.3	17.5	0.32	86	0.023	0.14	4.2	6.1	1700	45.0
13	550	53.3	20.2	0.37	90	0.022	0.16	5.1	7.4	1700	36.5
14	450	59.0	23.7	0.44	88	0.025	0.21	5.7	8.5	1900	24.5
15	525	59.0	20	0.36	85	0.026	0.16	4.6	6.3	1900	33.2
16	600	59.0	17.8	0.32	86	0.026	0.14	4.1	5.5	1900	43.6
17	450	64.2	23.5	0.43	87	0.028	0.23	5.4	8.2	2000	24.5
18	525	64.2	19.8	0.36	84	0.029	0.18	4.4	6.2	2000	33.2
19	600	64.2	18	0.32	87	0.028	0.15	4.0	5.4	2000	43.6
20	440	71.0	24	0.44	87	0.030	0.23	5.3	7.7	2200	23.6
21	525	71.0	20	0.36	85	0.031	0.19	4.3	6.1	2200	33.2
22	625	71.0	16.5	0.30	82	0.032	0.16	3.4	4.8	2200	47.2
23	575	76.2	18.7	0.34	87	0.033	0.18	3.8	5.6	2400	40.0

REFERENCE

1. Binnie, A. M., Experiments on the Swirling Flow of Water in a Vertical Pipe and a Bend, Proc. Roy. Soc. A, Vol 270, pp. 452-466, 1962.

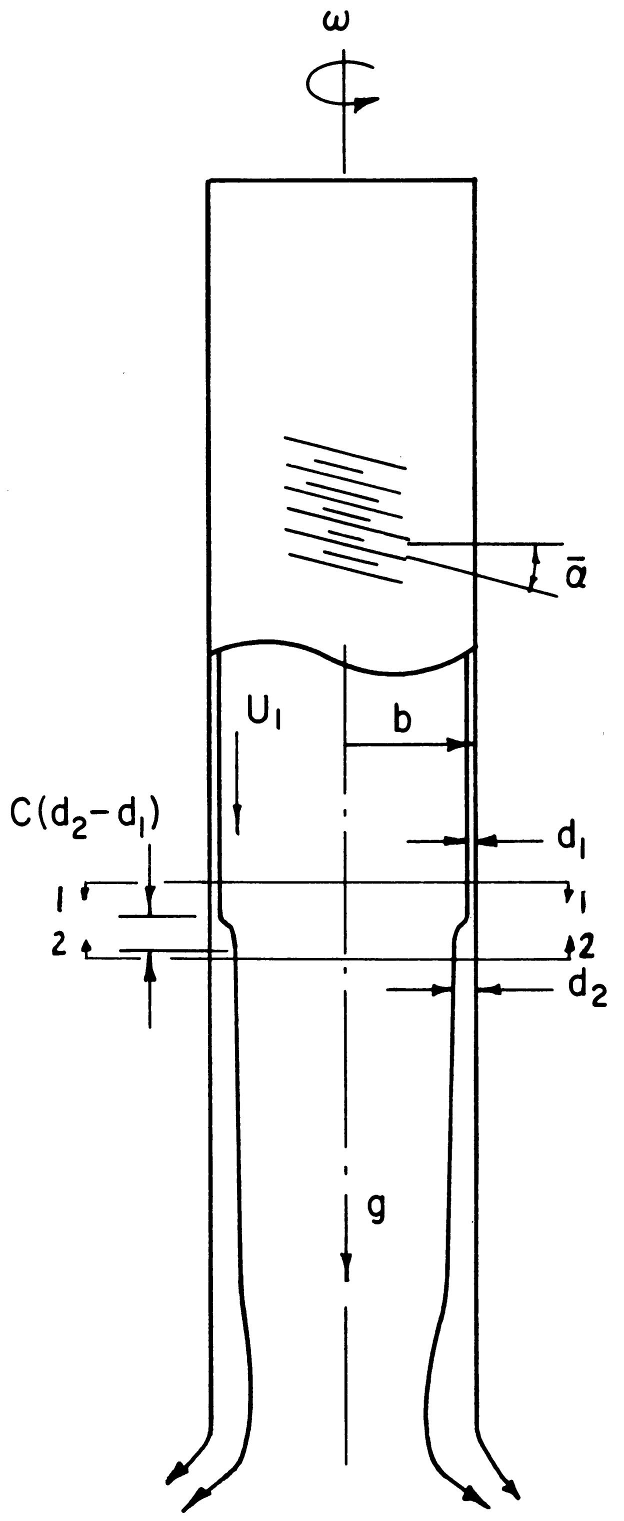

Figure 1. Definition sketch.

1. Supporting structure
2. Flowmeters
3. Depth indicator scale
4. Seal
5. Rotating union
6. Flange bearing
7. Circular flow spreader plate
8. Top hub sleeve bearing
9. Cast resin transparent tube
10. Center post assembly
11. Depth gages
12. Control tube
13. Bevel gearing
14. Flow controller
15. Efflux port
16. Collection box
17. Turntable
18. Turntable spindle
19. Drive belt and pulley
20. Input shaft of right angle drive
21. Magnetic pick-up
22. Electronic counter
23. Shaft extension
24. Threaded nut assembly
25. Structure base
26. Leveling screws and pads

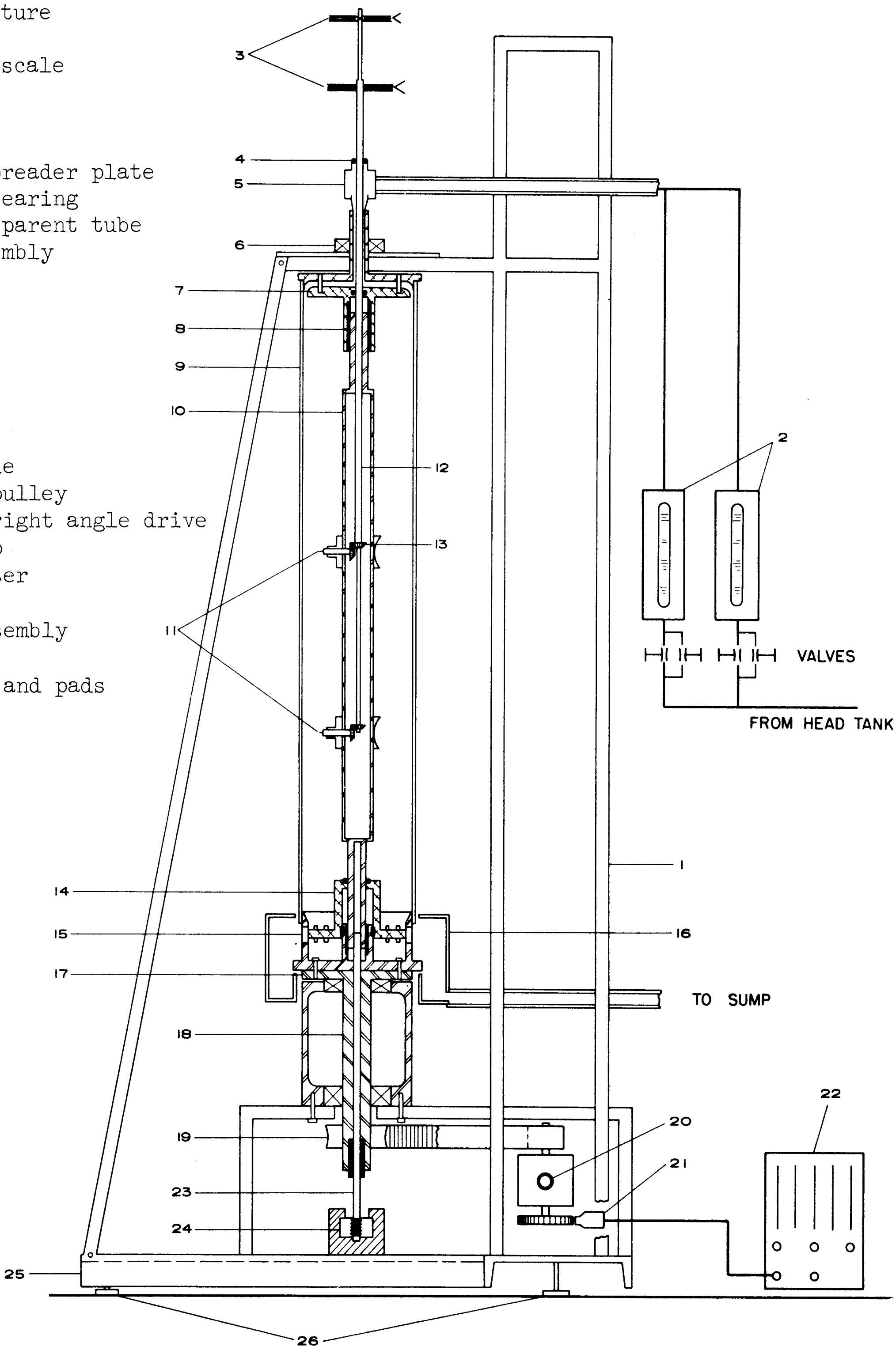

Figure 2. Schematic diagram of the apparatus.

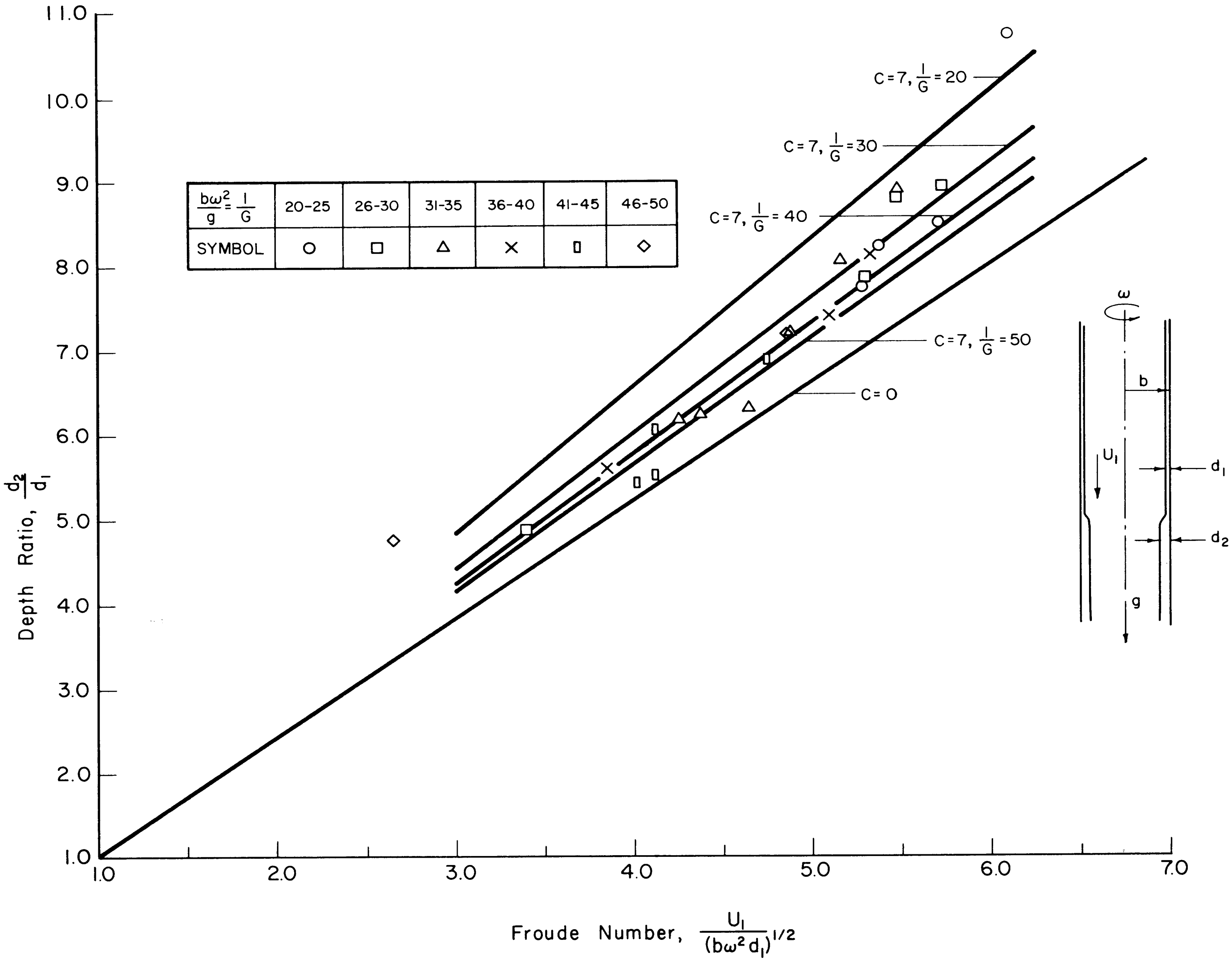

Figure 3. Comparison of theoretical and experimental results.

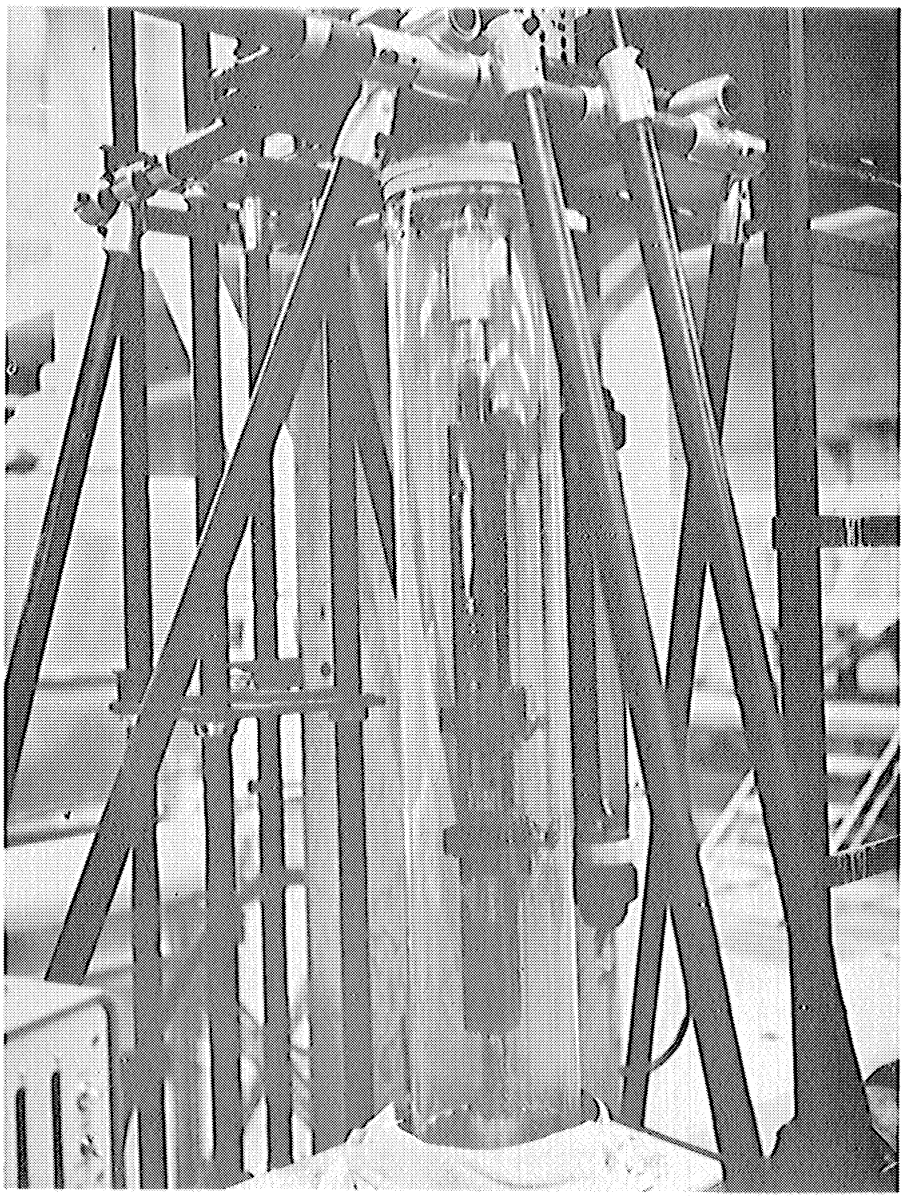

Plate 1. A photograph of the apparatus used.

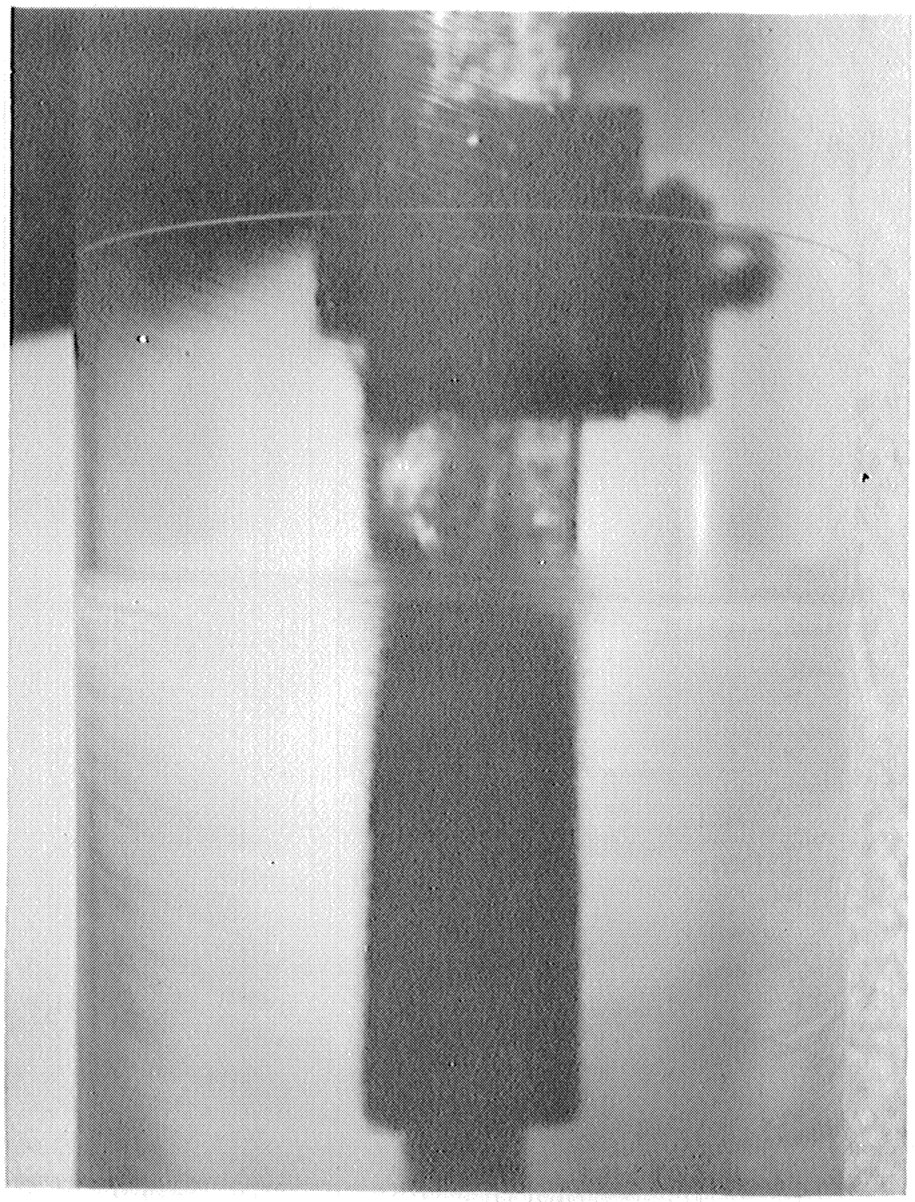

Plate 2. A photograph showing location of the jump and streaks in the flow.